Revista Ingeniería Biomédica
ISSN 1909-9762 / Volumen 8 / Número 15 / Enero-Junio de 2014 / pp.27-35
Escuela de Ingeniería de Antioquia-Universidad CES / Envigado, Colombia

The Effects of Time and Moisture on Elasticity Imaging Phantom Physical and Mechanical Properties: A Pilot Study

Andre Matthew Loyd [1, Ψ], Carolina Amador [2], Kai-Nan An [1],

[1] *Division of orthopedic research, Mayo Clinic, Rochester, United States*
Biomechanics Laboratory
[2] *Department of Physiology & Biomedical Engineering, Mayo Clinic, Rochester, United States*
Ultrasound Research Laboratory

Recibido 22 de agosto de 2013. Aprobado 18 de marzo de 2014

Efectos de tiempo y humedad en las propiedades mecánicas y físicas de un fantoma de imágenes de elasticidad: estudio piloto

Efeitos do tempo e umidade nas propriedades mecânicas e físicas de uma fantoma de imagenes de elasticidade: um estudo piloto

Abstract — Elasticity imaging phantoms are used to mimic human tissue as a means of testing and validating non-invasive techniques for measuring mechanical properties of human tissues. Limited studies of phantom stability have shown that phantom stiffness change over time when exposed to air. The goals of this study were to investigate how the physical and mechanical properties of elasticity imaging phantoms change with time and moisture state.

Two moisture states were tested; a dry state where the phantom was exposed to open air and a wet state where the phantom was submerged in water for 480 minutes. Polyvinyl alcohol (PVA) phantoms (cylindrical shape) were used. The properties of the phantom were found using flat indentation tests and a test battery that included a precondition test, a 0.05 mm/s triangle test, a 5 mm/s triangle test and a ten-second ramp-and-hold relaxation test. This battery was done at multiple time points: 0, 15, 30, 45, 60, 120, 180, 240, 360 and 480 minutes. At each time point, the modulus, stiffness and relaxation at 10 seconds were calculated. In addition, the mass and volume of the phantoms were measured at each time point.

The physical and mechanical properties of the phantoms were found to be statistically dependent on moisture state and time ($p<0.05$). The stiffness and moduli of the dry samples increased with time while the mass and volume decreased with time. Additionally, a strong correlation was found between the change in mass and change in modulus/stiffness for the dry phantoms. For the wet samples, the modulus and stiffness decreased with time while the mass and volume increase with time. The properties of the phantom begin to change within 15 minutes, the percentage change of the mechanical and physical properties remained, on average, under 10% during the first hour and increased up to 50% during 8 hours. These property changes of phantoms should be considered when using phantoms to test or validate non-invasive techniques.

Ψ Dirección para correspondencia: andre.m.loyd@gmail.com
DOI: http:/dx.doi.org/10.14508/rbme.2014.8.15.27-35

***Keywords*—** Elasticity imaging; Elasticity; Phantoms; Mechanical test.

***Resumen*—** Fantomas de imágenes de elasticidad se utilizan para imitar el tejido humano como un medio de ensayo y validación de técnicas no invasivas para medir las propiedades mecánicas de los tejidos humanos. La estabilidad de los fantomas se ha estudiado anteriormente y se ha encontrado que su elasticidad cambia con respecto al tiempo cuando están expuestas al aire. Los objetivos de este estudio fueron investigar cómo las propiedades físicas y mecánicas de los fantomas de imágenes de elasticidad cambian con el tiempo y el estado de humedad.

Dos estados de humedad fueron examinados; un estado seco, donde el fantoma se expone al aire libre y un estado húmedo, donde el fantoma se sumergió en el agua. Se utiliza alcohol polivinílico (PVA) para crear los fantomas (forma cilíndrica). Las propiedades del fantoma se encontraron utilizando pruebas de indentación planas y una batería de pruebas que incluyeron una prueba de condición, a 0.05 mm/s prueba triangular, una prueba triangular 5 mm/s, y ensayo de relajación de rampa-retención de diez segundos. Esta batería se realiza en múltiples puntos de tiempo: 0, 15, 30, 45, 60, 120, 180, 240, 360 y 480 minutos. En cada punto de tiempo, se calcularon el módulo, la rigidez y la relajación en 10 segundos. Además, la masa y el volumen de los fantomas se midieron en cada punto de tiempo.

Se encontró que las propiedades físicas y mecánicas de los fantomas son dependientes estadísticamente del estado de humedad y el tiempo ($p < 0,05$). La rigidez y módulos de las muestras secas se incrementaron con el tiempo mientras que la masa y el volumen disminuyó con el tiempo. Adicionalmente, una fuerte correlación fue encontrada entre los cambios de masa respecto al cambio de módulo para las muestras secas. Para las muestras húmedas, el módulo y la rigidez disminuyeron con el tiempo, mientras que aumentó la masa y el volumen con el tiempo. Las propiedades de los fantomas comienzan a cambiar dentro de los 15 minutos, pero el porcentaje de cambio de las propiedades mecánicas y físicas se mantuvo, en promedio, menos del 10% durante la primera hora y aumentó hasta el 50% en las 8 horas. Estos cambios en las propiedades de los fantomas deben ser considerados cuando se utilizan para probar o validar las técnicas no invasivas.

***Palabras claves*—** Fantomas; Imágenes de elasticidad; Elasticidad; Ensayo mecánico.

***Resumo*—** Fantomas de imagenes de elasticidade foram utilizadas para imitar o tecido humano como um meio de testes e validação de técnicas não invasivas para medir as propriedades mecânicas dos tecidos humanos. A estabilidade dos fantomas foi estudada previamente e descobriram que a elasticidade se altera com o tempo quando é exposta ao ar. Os objetivos deste estudo foram investigar como as propriedades físicas e mecânicas dos fantomas de imagem de elasticidade mudam ao longo do tempo e o estado de umidade.

Dois estados de umidade foram examinados; um estado de seca, em que o fantoma está exposta ao ar livre e um estado úmido, onde o fantoma foi imersa em água. é usado Álcool polivinílico (PVA) para criar o fantoma (forma cilíndrica). As propriedades do fantoma foram encontrados por meio de testes de indentação planas e uma bateria de testes, incluindo um teste de condição, a 0,05 mm / s teste triangular, um teste triangular de 5 mm / s, e teste de relaxamento rampa de Retenção de dez segundos. Esta bateria é realizada em vários pontos de tempo: 0, 15, 30, 45, 60, 120, 180, 240, 360 e 480 minutos. Em cada ponto de tempo, foram calculados o módulo de elasticidade, rigidez e relaxamento em 10 segundos,. Além disso, a massa e volume dos fantomas foram medidos em cada ponto de tempo. Verificou-se que as propriedades físicas e mecânicas dos fantomas são dependentes estatisticamente do estado de umidade e tempo ($p < 0,05$). A rigidez e módulos das amostras secas aumentou com o tempo, enquanto a massa e volume diminuiu com o tempo. Além disso, foi encontrada uma forte correlação entre as alterações na massa com respeito à alteração do módulo para amostras secas. Para as amostras molhadas, o módulo de elasticidade e rigidez diminuiu ao longo do tempo, enquanto o aumento da massa e do volume ao longo do tempo. As propriedades dos fantomas começam a mudar dentro dos 15 minutos, mas a percentagem de variação das propriedades mecânicas e físicas permaneceram, em média, menos de 10% durante a primeira hora, e aumentou até 50% em 8 horas. Essas alterações nas propriedades dos fantomas deve ser considerado quando é usado para testar ou validar as técnicas não invasivas.

***Palavras-chave*—** Fantomas; Imagens de elasticidade; Elasticidade; Teste mecânico.

I. Introduction

The measuring of mechanical properties of human tissue is a means of identifying healthy and unhealthy tissue [1]. Numerous elasticity imaging techniques, such as Shear Wave Elasticity Imaging (SWEI) [2], Acoustic Radiation Force Imaging (ARFI) [3], Transient Elastography (TE) [4], Magnetic Resonance Elastography (MRE) [5], Supersonic Shear Imaging (SSI) [6] and Shearwave Dispersion Ultrasound Vibrometry (SDUV) [7], are being developed to more accurately identify mechanical properties of human tissue non-invasively. Researchers rely on tissue mimicking phantoms to develop and test novel techniques. Phantoms are used because they mimic the mechanical properties and density of human tissues and are inexpensive [8]. Phantoms are used to check the accuracy and validate mechanical property measurements.

Several methods to measure tissue mechanical properties such as stress-relaxation, quasi-static and dynamic test have been used on biological tissues [9]. Mechanical tests had been used to evaluate the accuracy of elasticity methods such as MRE, ARFI, SDUV and TE. MRE measurements have been compared to compression

tests and dynamic tests on tissue like gelatin phantoms of varying elasticity [10, 11]. An integrated indentation and ARFI imaging has been used to characterize soft tissue stiffness [12]. SDUV estimation of shear elastic modulus has been compared to indentation test in gelatin phantoms [13]. TE measurements have been compared to tensile tests and dynamic test on a tissue like polymers [14, 15]. Cross-validation between MRE and ultrasound-based transient elastography had been made in homogeneous tissue mimicking phantoms [16, 17]. Dynamic tests allow estimation of the change in tissue property parameters versus frequency, but the material needs to be characterized one frequency at a time. Quasi-static methods include compression tests, tensile tests and indentation tests. Compared to the others, indentation tests have been widely used to assess the mechanical properties of tissues. Their main advantage is that they can be applied both ex vivo and in vivo [18-27]. The indentation test is considered a gold standard test to assess elastic mechanical properties. Furthermore, it is attractive because of its widespread use and ease of implementation, with its only requirement is to have a surface for indenter contact application.

Water based phantom stability have been studied in the field of Nuclear Magnetic Resonance (NMR) and ultrasound Elastography. Medsen et al. [28] studied two phantoms with the same composition at 14 and 20 weeks after manufacture, there was limited evidence of the long-term stability measured by NMR. In the area of ultrasound Elastography, Korte et al. [29] reported evidence of influence of aging in the compression modulus of water based phantoms measured by Dynamic Mechanical Analysis (DMA), Hall et al. [30] studied the compression modulus of gelatin phantoms over 246 days and found that phantom stiffness increases with time. The overall conclusion in these studies is that the mechanical properties of water based phantoms when exposed to air increase with time and this may be due to an osmotic mechanism.

Although there are studies concerning the mechanical properties of tissue mimicking phantoms when exposed to air over time, there are no studies that discuss the stability of phantoms under moisture conditions. Moreover, there is a strong concern on reproducibility of the data and therefore phantom stability studies are needed. The Radiological Society of North America (RSNA) recently created the Quantitative Imaging Biomarkers Alliance (QIBA) [31] for Elastography methods, where tissue-mimicking phantoms are being study by several ultrasound elastography methods to evaluate reproducibility and stability of the methods. Hence, the goal of this study is to investigate how the physical and mechanical properties of elasticity imaging phantoms change with time and moisture conditions. The phantoms will be tested in two conditions: submerged in water (wet) and expose the air (dry). It is hypothesized that the phantoms mechanical properties will change with time, moreover the mass and volume of the wet samples will increase with time and the mass and volume will decrease for the dry samples.

II. Materials and Methods

2.1 Phantoms

Polyvinyl alcohol (PVA) phantoms (cylindrical shape) were used and were made using PVA (powder form from Sigma-Aldrich, St. Louis, MO). A solution consisting of 10% PVA powder (by volume) was mixed at room temperature in a solvent of 70% distilled water. A preservative of potassium sorbate (Sigma-Aldrich, St. Louis, MO) was added with concentration of 10% by volume. Cellulose particles (Sigma-Aldrich, St. Louis, MO) with size of 20 μm were also added with a concentration of 1% by volume to provide adequate ultrasonic scattering. A gelling agent, polyethylene glycol (PEG) was added by 30 % concentration (liquid form from Sigma-Aldrich, St. Louis, MO). The solution was stirred for 1 hour at 90°C, degassed and poured into cylindrical-shape molds that exceeded the diameter of 50 mm and height of 60 mm. After samples reached room temperature, they were subject to 1 thermal cycle, which involved cooling from room temperature to -17°C, staying at -17°C for 24 hours, then place at room temperature for 12 hours.

At total of ten cylinder-shaped phantom were made; each had diameters that exceeded 50 mm and heights of 60 mm. The phantoms were placed into one of two moisture states: "wet" where the phantoms were submerged in water or "dry" where the phantoms were exposed to open air. Five phantoms were placed into each moisture state. Two different types of tests were run on the samples: mechanical tests where the stiffness, modulus and relaxations were measured and physical tests where the mass and volume were measured. Each sample used to conduct mechanical tests, physical tests or both.

2.2 Mechanical Tests

The compression tests were done using a flat-cylindrical aluminum indenter. The radius of the indenter was 3.15 mm to insure that the phantom diameter and height were both 15 times larger than the indenter radius as recommended by Zhai et al. [32]. The testing was conducted using a Bose Electroforce 3200 (Eden Prairie, MN) actuator. The force was measured using a 5 lb Honeywell (Morristown, NJ) miniature load cell. The displacement was measured using the Bose Electroforce 3200 internal linear variable differential transformer (LVDT). The data was collected using LabVIEW (National Instruments; Austin, TX).

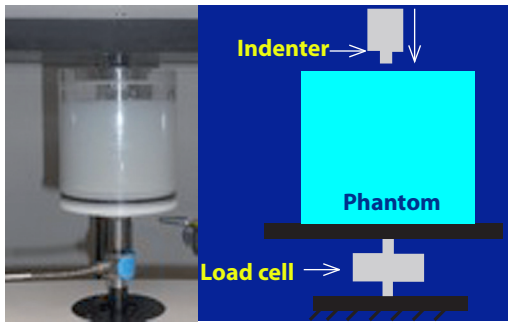

Fig. 1. Picture and schematic of the test setup for the phantom indentation tests. The indenter was a flat cylinder with a 3.15 mm radius. The picture shows a phantom submerged in water.

The indentation test battery included a precondition test, a static deflection test at 0.05 mm/s, a high-rate indentation tests at 5 mm/s and a relaxation test. For the precondition test, 1 Hz cyclic tests were done for 60 seconds with a maximum compression amount of 0.75 mm. The static deflection and high rate tests were triangle waves with compression amounts of 1.5 mm. The relaxation test had an initial ramp rate of 50 mm/s to 1.5 mm of compression and then a hold for 10 seconds (Table 1). The 1.5 mm maximum displacement was used to stay in the linear region of the force-displacement curve. 0.75 mm was used for the precondition because it was half of the maximum displacement. The complete battery of tests were repeated at different time points to investigate the effects of time. The tests were conducted at time points of 0 min, 15 min, 30 min, 45 min, 60 min, 120 min, 180 min, 240 min, 360 min. and 480 min.

Table 1. The test battery

Test	Actuator Action	Ramp Speed	Compression Amount (mm)	Frequency
Precondition	Sine wave	Not Apply	0.75	1 Hz for 60 sec
Static deflection	Triangle	0.05 mm/s	1.50	Not Apply
Fast rate	Triangle	5 mm/s	1.50	Not Apply
Relaxation	Ramp and hold	50 mm/s	1.50	Not Apply

2.2 Physical Properties

For the physical properties, the mass, diameter and height of the phantom sample were measured at each time point. The mass was measured using a digital scale and the diameter and height was measured using a ruler.

2.3 Analysis

All of the LabVIEW data was filtered using a Butterworth filter with a cut off frequency of 10 Hz. The compressive stiffness and modulus of elasticity were measured using indentation tests. The stiffness of the each sample was calculated using the slope of the force-displacement from 50% of the maximum displacement to the peak force. The modulus of elasticity was calculated using the peak force and Equation 1 where "v" and "R" were Poisson's ratio and indenter radius [32].

$$E = \frac{Force\left(1 - v^2\right)}{2R\,(Disp)} \quad (1)$$

The relaxation function (G(t)) was calculated from each relaxation test by normalizing all of the forces points by the peak force. G_{10} was found by taking the value of G(t) at ten seconds. The volume of the phantom was calculated using the volumetric equation for a cylinder and the diameter and height measurements. The percentage change was calculated for stiffness, modulus and G_{10} for each time point using the values at $t = 0$ as the reference values.

Results are reported as mean ± standard deviation. The number of samples, repetitions and fits were made on the basics of the data and the degree of scatter and reproducibility. Repeated measures analyses of covariance (ANCOVA) were used to evaluate the effect of time, ramp velocity and moisture on the percentage change of the modulus, compression stiffness, mass, volume and G_{10}. Tukey-Kramer analyses of the percentage change were used to evaluate the differences between each time point for each moisture state. Statistical significance for all tests was accepted for $p \leq 0.05$.

III. Results

3.1 Mechanical Properties

An example of the force displacement data that affirms that the compression of the phantoms was linear is shown (Fig. 2). Moreover, the force displacement data illustrate that the phantom is not rate dependent within 0 to 0.15 N.

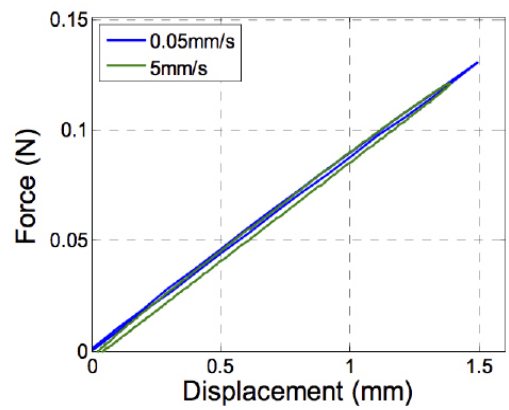

Fig. 2. Example of force-displacement measurements from 0.05 mm/s and 5 mm/s compression test with the phantom submerged in water.

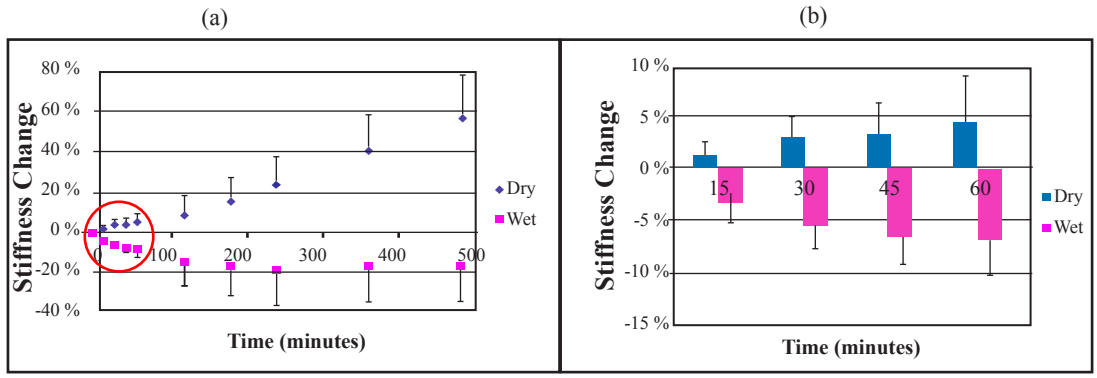

Fig. 3. Graphs showing stiffness of the phantoms change with time for each moisture state. The graph on the right is a close up view of the changes during the first hour.

The average (n=4 for each moisture state) stiffness change of the phantoms respect to the baseline measurement as a function of time for each moisture state, Fig. 3.

The repeated-measures ANCOVA showed that the modulus and stiffness were statistically dependent upon the moisture state and time ($p<0.05$). The changed in modulus results mirrored the results of the change in stiffness; the modulus increase for the dry state and decreased for the wet state, (Fig. 4).

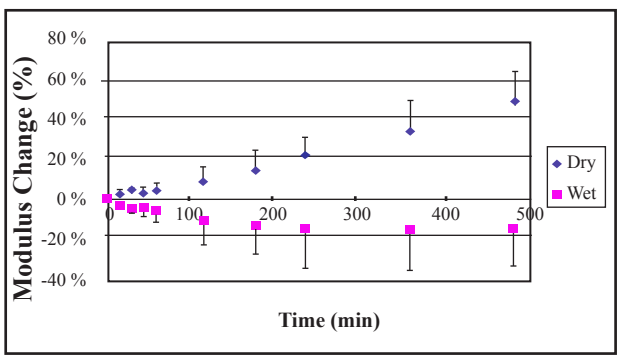

Fig. 4. The change in modulus over time being in a dry condition or being submerged in water. A repeated-measures

An example plot of a relaxation tests is shown in Fig. 5. The repeated-measures ANCOVA of the change in G_{10} showed that time was the only significant predictor ($p<0.001$), Fig. 6.

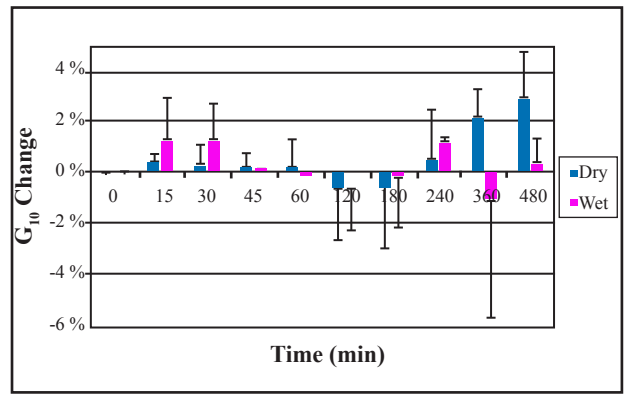

Fig. 6. Graph of the percentage change of G_{10} at each time point. The repeated-measures ANCOVA reported that time was the only significant factor. All of the average changes were less than 3%.

3.2 Physical Properties

The average mass change as a function of time for each moisture state is shown in Fig. 7.

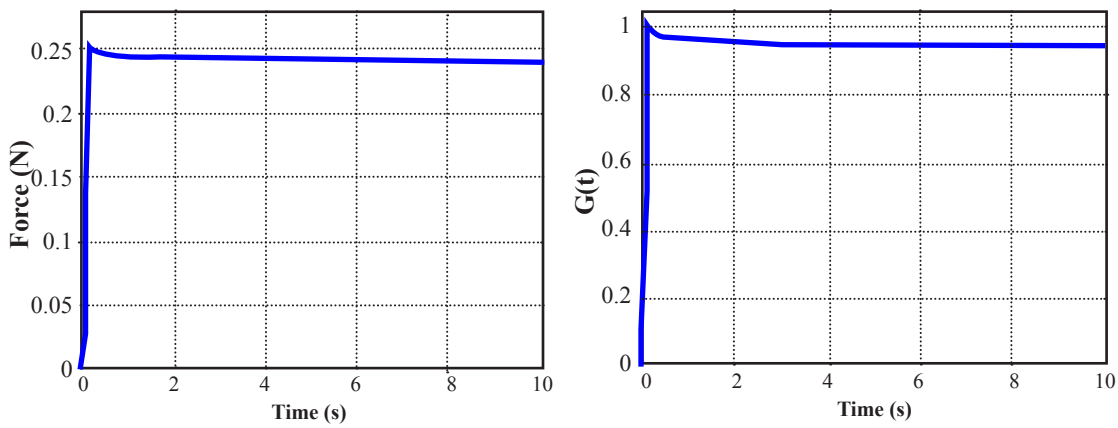

Fig. 5. Plot of the force-time curve (left) and the relaxation function G(t) (right) of a submerged relaxation tests.

The mass of the phantoms increased for the submerged phantoms and decreased for the dry phantoms. The repeated-measures ANCOVA showed that the moisture state and time were significant predictors of the change in mass. For both, moisture states the mass behaved in a steady fashion. The dry samples change in mass was modeled as a function of time (t, minutes) and found to be well represented by the expression:

$$Dry\ mass\ change\ (\%) = a * t + b \qquad (2)$$

where a = -1.679x10^{-2} and b = -0.26. The fit's adjusted R^2 was 0.9852 was and the both coefficients were statistically significant ($p<0.005$). There was no evidence of a lack of fit using Durbin-Watson statistic ($d = 0.4$ and $p<0.001$).

Similarly, the submerged samples' change of mass was modeled as a function of time (t, minutes) and found to be well represented by the expression:

$$Wet\ mass\ change = c * ln(t) + d \qquad (3)$$

where c = 2.47 and d = -5.61. The fit's adjust R^2 was 0.89 and both coefficients were statistically significant ($p<0.001$) and the model did not show evidence of lack of fit using Durbin-Watson statistic ($d = 0.4$ and $p<0.001$).

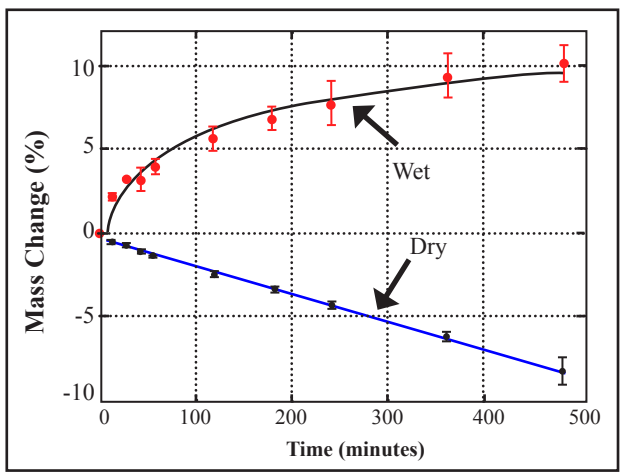

Fig. 7. Plot of the mass change by percentage for dry phantoms and phantoms submerged in water. The blue line shows the linear fit of the percentage mass decrease for the dry samples; the black line show the logarithmic fit of the percentage mass increase for the submerged samples. Note that the fits were done using the individual points not the averaged points.

The volume change of the phantoms were similar to the results found for the mass change. The wet phantoms increased in volume and the dry phantoms decreased in volume. The patterns can be seen in a plot of the results (Fig. 8). Even though the mass and volume properties were changed in conjunction with each other, the density was not constant for the phantoms. The density increased with time for the dry samples and decrease with time for the wet samples (Fig. 9).

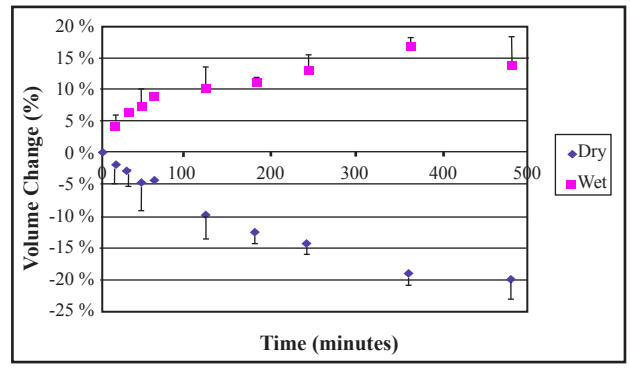

Fig. 8. Plot of the volume change by percentage for dry phantoms and phantoms submerged in water. A repeated-measures ANCOVA showed that the volume change was statistically dependent on the moisture state and time.

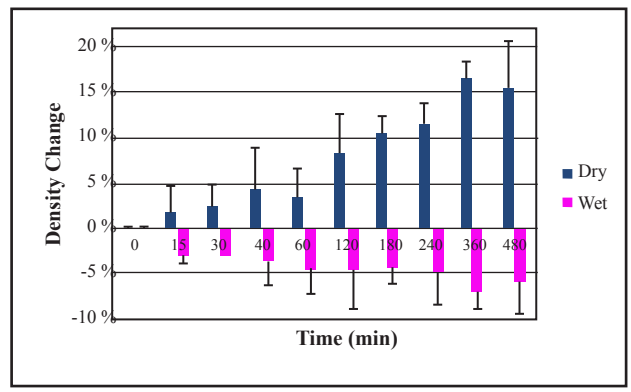

Fig. 9. Plot the density change by percentage for the dry phantoms and phantoms submerged in water.

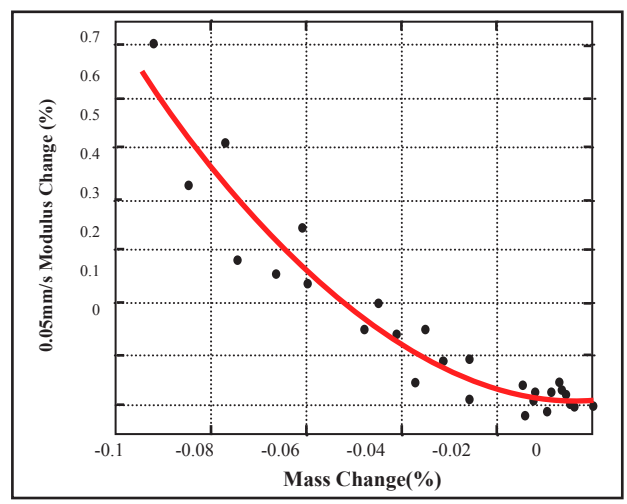

Fig. 10. Plot of the percentage dry modulus change for the 0.05 mm/s test versus the percentage mass change.

Tables II and III summarize the average mechanical properties and physical properties change respect to baseline.

Table 2. Dry samples

Time (min)	Density Change	Stiffness Change	Modulus Change	Mass Change	G10 Change
0	0.0%	0.0%	0.0%	0.0%	0.0%
15	1.7%	1.2%	1.2%	-0.5%	0.4%
30	2.4%	3.1%	3.5%	-0.7%	0.3%
45	4.2%	3.3%	1.7%	-1.1%	0.2%
60	3.4%	4.5%	3.3%	-1.4%	0.2%
120	8.3%	8.4%	8.3%	-2.4%	-0.7%
180	10.6%	15.0%	13.6%	-3.5%	-0.6%
240	11.5%	23.4%	20.7%	-4.5%	0.6%
360	16.5%	39.8%	35.1%	-6.2%	2.2%
480	15.4%	55.1%	48.4%	-8.2%	2.9%

Table 3. Wet samples

Time (min)	Density Change	Stiffness Change	Modulus Change	Mass Change	G10 Change
0	0.0%	0.0%	0.0%	0.0%	0.0%
15	-3.0%	-3.3%	-3.6%	2.1%	1.2%
30	-2.9%	-5.4%	-5.2%	3.2%	1.3%
45	-3.9%	-6.2%	-5.3%	3.2%	0.0%
60	-4.6%	-6.9%	-6.7%	4.0%	-0.1%
120	-4.7%	-14.9%	-12.7%	5.5%	-0.6%
180	-4.4%	-16.9%	-14.8%	6.8%	-0.1%
240	-5.1%	-18.8%	-16.5%	7.7%	1.2%
360	-6.9%	-17.2%	-17.2%	9.3%	-1.0%
480	-5.9%	-17.6%	-17.0%	10.1%	0.4%

A correlation was found between the change in stiffness and modulus, and the change in mass (Fig.10). For the dry phantoms, the decrease in mass resulted in non-linear increase in modulus and stiffness; the change in modulus as a function of change in mass was modeled well with a second degree polynomial:

$$Modulus\ change\ (\%) = e * \%MassChange^2 + f * \%MassChange + g$$

where $e = 73.785$, $f = 0.2223$, $g = 0.01$ and adjusted R^2 value of 0.92. No correlations between modulus and mass changes or stiffness and mass changes were seen for the wet samples.

IV. Discussion

PVA phantoms exhibit a linear force-displacement curve (Fig. 2) and there was no statistical difference when the phantoms were compress at 0.05 mm/s or 5 mm/s.

The results above show that phantoms that are exposed to air get stiffer with time and, in contrast, the phantoms submerged in water get more compliant with time, as shown in Fig. 3(a). The stiffness change as well as the modulus change for each condition was less than 10% until one hour had passed, Tables I and II.

The mechanical properties of the phantom started to change immediately. The dry phantoms loss mass, volume and gained in stiffness within fifteen minutes. This is probably due to the phantoms losing water over time; therefore increasing the concentration of the solvent in the phantom which increased the stiffness. This fact is supported by the fact that the density increased with time for the dry phantoms which is probably due to the increase in concentration of the solvent (Fig. 9). Submerging the phantoms in water had the opposite effect of what was seen in the dry phantoms. The wet phantoms gained mass and volume, yet decreased in stiffness and modulus. While submerged in water, the phantom likely gained water over time which decreased the concentration of the solvent in the phantom – therefore, decreasing the stiffness and the density. The added water probably caused the wet phantoms' volume and mass to increase over time.

However, a plot of the G_{10} over time showed that there was no clear G_{10} increase or decrease with time and that the change on average was less than 3% for each

time point. Studies in the literature have attributed these changes in mechanical properties over time to osmotic forces which causes fluid to migrate across the interface of difference materials [30]. For instance, in the case the phantom was submerged in water the diffusion forces may have cause water to migrate to the phantom and therefore increasing its weight and volume and decreasing its stiffness/modulus. For the case of phantom exposed to air, a diffusion process may the phantom dehydration and therefore its loss of weight and volume and increase in stiffness and modulus.

A relationship was identified between change in mass and change in modulus/stiffness for the dry samples. The decrease in mass was directly related to an increase in modulus that could be fitted closely with an equation. This could provide guidance to predict changes in modulus that could occur over time if the mass is being monitored.

The relaxation data showed that the changes in the amount of relaxation was small (less than 3%) and did not vary with moisture content. This small variability could be due to the small amount of relaxation these phantoms display. The vast majority of the samples had G_{10} that were greater than 0.9.

This study shows that properties of phantoms are a function of time whether submerged in water or exposed to air. This factor should be taken into account when conducting experiments on phantoms where the accuracy of the modulus of elasticity or stiffness is important.

The range of initial modulus of elasticity for these phantoms was 16 to 40 kPa, hence the factor should apply to phantoms that have moduli of elasticity within this range. For tests where a ten percent change is acceptable, then completing testing of the phantom within an hour is essential. For tests where the phantom properties should be constant, the testing should be completed within fifteen minutes. The mass and volumetric equations provide estimates of how the phantom will change and can be used to account for changes during experimentation. Additionally, the change in modulus and change in mass correlations could be used to predict the changed in modulus during experimentation

4.1 Limitations

There are limitations to this study. First, this study only measured the phantom stiffness and relaxation using mechanical means. This study should be repeated by using an elasticity imaging method to measure the modulus of elasticity and relaxation. Second, only one type of phantom was used. Third, this study did not control the time that elapsed between when the phantom was created and the phantom was tested. Another limitation is that the test time was limited to 8 hours. Lastly, the indentation tests used a large indenter; however, care was taken so that all of the compression was in the linear region of the force-displacement curve. Additionally, the indenter's radius was less that 7% of the diameter and height of the phantom [32].

V. Conclusion

The physical and mechanical properties of the phantoms were found to change with time and moisture state. When a phantom was exposed to open air, the mass and volume decreased and the modulus of elasticity and stiffness increased with time. When a phantom is submerged in water, the mass and volume increased and the modulus of elasticity and stiffness decreased with time. For the phantoms exposed to open air, the change in mass can be used to predict the change in modulus. The relaxation properties of the phantom was unaffected by moisture state or time. The properties of the phantom were found to begin to change within 15 minutes, however the percentage change of the mechanical and physical properties on average remain under 10% during the first hour. These changes to the properties of phantoms should be considered when using phantoms to test or validate non-invasive techniques to estimate mechanical properties.

References

[1]. Skovoroda A., Klishko A., Gusakyan D. Quantitiative analysis of the mechanical characteristics of pathologically changed soft biological tissues. *Biophysics*, 40, 1359-1364, 1995 1995.

[2]. Sarvazyan A. P., Rudenko O. V., Swanson S. D., Fowlkes J. B., Emelianov S. Y. Shear wave elasticity imaging: A new ultrasonic technology of medical diagnostics. *Ultrasound Med. Biol.*, 24, 1419-1435, 1998.

[3]. Nightingale K. R., Palmeri M. L., Nightingale R. W., Trahey G. E. On the feasibility of remote palpation using acoustic radiation force. *Journal of the Acoustical Society of America*, 110, 625-634, Jul 2001.

[4]. Arndt R., Schmidt S., Loddenkemper C., Grünbaum M., Zidek W., Van Der Giet M., Westhoff T. H. Noninvasive evaluation of renal allograft fibrosis by transient elastography – a pilot study. *Transplant International*, 23, 871-877, 2010.

[5]. Muthupillai R., Lamos D. J., Rossman P. J., Greenleaf J. F., Manduca A., Ehman R. L. Magnetic resonance elastography by direct visualization of acoustic strain waves. *Science*, 269, 1854-1857, 1995.

[6]. Bercoff J., Tanter M., Fink M. Supersonic shear imaging: a new technique for soft tissue elasticity mapping. *IEEE Transactions on Ultrasonics Ferroelectrics and Frequency Control*, 51, 396-409, 2004.

[7]. Chen S., Urban M., Pislaru C., Kinnick R., Yi Z., Aiping Y., Greenleaf J., Shearwave dispersion ultrasound vibrometry (SDUV) for measuring tissue elasticity and viscosity. *IEEE Transactions on Ultrasonics Ferroelectrics and Frequency Control*, 56, 55-62, 2009.

[8]. Madsen E. L., Zagzebski J. A., Banjavie R. A., Jutila R. E. Tissue mimicking materials for ultrasound phantoms. *Am. Assoc. Phsys. Med*., 5, 391-394, Sep./Oct. 1978.

[9]. Fung Y. Biomechanics: mechanical properties of living tissues: Springer-Verlag, 1993.

[10]. Hamhaber U., Grieshaber V. A., Nagel J. H., Klose U. Comparison of quantitative shear wave MR-elastography with mechanical compression tests. *Magnetic Resonance in Medicine*, 49, 71-77, Jan 2003.

[11]. Ringleb S. I., Chen Q. S., Lake D. S., Manduca A., Ehman R. L., An K. N. Quantitative shear wave magnetic resonance elastography: Comparison to a dynamic shear material test. *Magnetic Resonance in Medicine*, 53, 1197-1201, May 2005.

[12]. Zhai L., Palmeri M. L., Bouchard R. R., Nightingale R. W., Nightingale K. R. An integrated indenter-ARFI imaging system for tissue stiffness quantification. *Ultrasonic Imaging*, 30, 95-111, 2008.

[13]. Amador C., Urban M. W., Chen S., Chen Q., An K., Greenleaf J. F. Shear Elastic Modulus Estimation From Indentation and SDUV on Gelatin Phantoms. *Biomedical Engineering, IEEE Transactions on*, 58, 1706-1714, 2011.

[14]. Fromageau J., Gennisson J. L., Schmitt C., Maurice R. L., Mongrain R., Cloutier G. Estimation of polyvinyl alcohol cryogel mechanical properties with four ultrasound elastography methods and comparison with gold standard testings. *IEEE Transactions on Ultrasonics Ferroelectrics and Frequency Control*, 54, 498-509, Mar 2007.

[15]. Oudry J., Bastard C., Miette V., Willinger R., Sandrin, L. Copolymer-in-oil phantom materials for elastography. *Ultrasound in Medicine and Biology*, 35, 1185-1197, Jul 2009.

[16]. Oudry J., Vappou J., Choquet P., Willinger R., Sandrin L., Constantinesco A. Ultrasound-based transient elastography compared to magnetic resonance elastography in soft tissue-mimicking gels. *Physics in Medicine and Biology*, 54, 6979-6990, Nov 2009.

[17]. Oudry J., Chen J., Glaser K. J., Miette V., Sandrin L., Ehman R. L. Cross-Validation of Magnetic Resonance Elastography and Ultrasound-Based Transient Elastography: A Preliminary Phantom Study. *Journal of Magnetic Resonance Imaging*, 30, 1145-1150, Nov 2009.

[18]. Fung Y. C. in *Biomechanics: Mechanical Properties of Living Tissues*, ed: Springer-Verlag, 1993.

[19]. Al-ja'afreh T., Zweiri Y., Seneviratne L., Althoefer K. A new soft-tissue indentation model for estimating circular indenter 'force-displacement' characteristics. *Proceedings of the Institution of Mechanical Engineers Part H Journal of Engineering in Medicine*, 222, 805-815, 2008.

[20]. Paillermattei C., Bec S., Zahouani H. In vivo measurements of the elastic mechanical properties of human skin by indentation tests. *Medical Engineering & Physics*, 30, 599-606, 2008.

[21]. Carter F. J., Frank T. G., McLean D., Cuschieri A. Measurements and modeling of the compliance of human and porcine organ. *Med. Image Anal*., 5, 231-236, 2001.

[22]. Miller K., Chinzei K., Orssengo G., Bednarz P. Mechanical properties of brain tissue : Experiment and computer simulation. *J. Biomech.*, 33, 1369-1376, 2000.

[23]. Kim J., Srinivasan M. A. Characterization of Viscoelastic Soft Tissue Properties from In Vivo Animal Experiments and Inverse FE Parameter Estimation. *Medical Image Computing and Computer-Assisted Intervention - MICCAI,* ed: Springer-Verlag, 3750, 599-606, 2005.

[24]. Tay B. K., Kim J., Srinivasan M. A. In Vivo Mechanical Behavior of Intra-abdominal Organs. I*EEE Transactions on Biomedical Engineering*, 53, 2129-2138, 2006.

[25]. Schwartz J. M., Denninger M., Rancourt D., Moisan C., Laurendeau D. Modeling liver tissue properties using a on-linear viscoelastic model for surgery simulation. *Med. Imag. Anal.*, 9, 103-112, 2005.

[26]. Samur E., Sedef M., Basdogan C., Avtan L., Duzgun O. A robotic indenter for minimally invasive measurement and characterization of soft tissue response. *Medical Image Analysis*, 11, 361-373, 2007.

[27]. Ahn B., Kim J. Measurement and characterization of soft tissue behavior with surface deformation and force response under large deformations. *Medical Image Analysis*, 14, 138-148.

[28]. Madsen E. L., Blechinger J. C., Frank G. R. Low-contrast focal lesion detectability phantom for H-1 MR imaging. *Medical Physics*, 18, 549-554, May-Jun 1991.

[29]. DeKorte C. L., Cespedes E. I., vanderSteen A. F. W., Norder B., Nijenhuis K. T. Elastic and acoustic properties of vessel mimicking material for elasticity imaging. *Ultrasonic Imaging*, 19, 112-126, Apr 1997.

[30]. Hall T. J., Bilgen M., Insana M. F., Krouskop T. A. Phantom materials for elastography. *IEEE Transactions on Ultrasonics Ferroelectrics and Frequency Control*, 44, 1355-1365, Nov 1997.

[31]. Radiological Society of North America: Quantitative Imaging Biomarkers Alliance. Consulted on April 1th, 2014 in: http://www.rsna.org/QIBA.aspx

[32]. Zhai L., Palmeri M. L., Bouchard R. R., Nightingale R. W., Nightingale K. R. An Integrated Indenter-ARFI Imaging System for Tissue Stiffness Quantification. *Ultrasound Imaging*, 30, 95-111, April, 2008 2008.